Peripapillary Microvascular and Neural Changes in Diabetes Mellitus: An OCT-Angiography Study

Stela Vujosevic,[1] Andrea Muraca,[1] Valentina Gatti,[1] Luca Masoero,[2] Marco Brambilla,[3] Barbara Cannillo,[3] Edoardo Villani,[4,5] Paolo Nucci,[4,5] and Stefano De Cillà[1,6]

[1]Eye Unit, University Hospital Maggiore della Carita', Novara, Italy
[2]Medical School, University East Piedmont "A. Avogadro", Novara, Italy
[3]Medical Physics, University Hospital Maggiore della Carità, Novara, Italy
[4]University Eye Clinic San Giuseppe Hospital, Milan, Italy
[5]Department of Clinical Science and Community Health, University of Milan, Milan, Italy
[6]Department of Health Science, University East Piedmont "A. Avogadro", Novara, Italy

Correspondence: Stela Vujosevic, University Hospital Maggiore della Carità, Eye Unit, Corso Mazzini 18, 28100 Novara; stela.vujosevic@gmail.com.

Submitted: May 27, 2018
Accepted: September 19, 2018

Citation: Vujosevic S, Muraca A, Gatti V, et al. Peripapillary microvascular and neural changes in diabetes mellitus: an OCT-angiography study. *Invest Ophthalmol Vis Sci*. 2018;59:5074–5081. https://doi.org/10.1167/iovs.18-24891

Purpose. To evaluate peripapillary vessel density and morphology in patients with diabetes mellitus (DM) without clinical signs of diabetic retinopathy (DR) and with mild, non-proliferative DR and to correlate with peripapillary nerve fiber layer (NFL) thickness.

Methods. One hundred seventeen eyes (34 healthy controls, 54 patients with DM without DR [noDR group] and 24 patients with mild DR [DR group]) were prospectively evaluated. All subjects underwent peripapillary and macular optical coherence tomography angiography (OCT-A). Peripapillary NFL thickness was also recorded. OCT-A slab of radial peripapillary plexus (RPC) and macular superficial capillary plexus (SCP) were analysed in order to calculate perfusion density (PD) and vessel density (VD). Further an image analysis of RPC slab was performed to identify number of branches (NoB) and total branches length (tBL).

Results. In peripapillary area there was a significant decrease in VD ($P = 0.003$), NoB ($P < 0.001$), and tBL ($P < 0.001$) in noDR group versus controls; PD values were not different among groups ($P = 0.126$); there was a significant decrease in average NFL thickness in DR versus controls ($P = 0.008$) and in the inferior quadrant in noDR group versus controls ($P = 0.03$); there was a significant correlation between OCT-A and NFL thickness values (ρ ranging from 0.19–0.57). In macular region PD and VD were decreased only in DR group ($P < 0.05$).

Conclusions. There are early changes in the peripapillary vessel morphology and VD of the RPC in patients with DM without DR that correlate to NFL thinning. Earlier changes in superficial vessel density are documented in the peripapillary than in the macular region. These data may confirm a coexistence of an early neuronal and microvascular damage in patients with DM without clinical signs of DR.

Keywords: oct-angiography, diabetes mellitus, peripapillary, microvascular, nerve fiber layer

Diabetic retinopathy (DR) is the leading cause of visual impairment in patients with diabetes mellitus (DM).[1] DM affects all cell types in the retina, as reported by numerous experimental and clinical studies.[2–7] At the microvascular level, modifications on pericytes and basement membrane, and endothelial cell loss ultimately lead to the alterations of the blood–retinal barrier.[8,9] There are microglial cell activation and neuronal apoptosis in the retina in DM.[3,4,10–15] In the peripapillary region, in patients with DM, these neural alterations can be clinically documented as a reduction of the retinal nerve fiber layer (NFL) thickness.[16–19]

The radial peripapillary capillary plexus (RPC), present only in the peripapillary region, has an important role in maintaining neuronal health.[20–22] RPC has straight and long vessels with no frequent anastomoses, as documented by histology.[21] Previously, fluorescein angiography was used to image this vascular structure; however, this is an invasive technique that only produces images of total vascularization, obscuring the details of individual vascular layers. Optical coherence tomography angiography (OCT-A) is a noninvasive and reproducible imaging technique, which has recently been used to study macular and peripapillary vascular structure with a heretofore impossible level of detail and clarity.[23–25] Different authors have used OCT-A to evaluate vascular density of RPC in healthy humans and in subjects with glaucoma.[26–33] No quantitative data are currently available on microvascular alterations in the peripapillary area in patients with DM. In this population, the density of vascular structures was evaluated with OCT-A only in the macular region.[34–37] Dimitrova et al.[34] have measured vessel density in superficial and deep capillary plexuses in the macula, reporting a decrease in density in patients with DM without DR as compared with healthy subjects. Kim et al.[35] added to this vascular density measurement, an evaluation of the vascular morphology and complexity in patients with DR, finding alterations of these parameters with the worsening of DR.

To the best of our knowledge, there are no studies that describe vascular density of RPC and its morphology in patients with DM.

The purpose of this study was to evaluate the features of the RPC in the peripapillary region in patients with DM without

clinical signs of DR and with mild nonproliferative DR and to correlate it with peripapillary NFL thickness.

Materials and Methods

Patients and Study Design

In this cross-sectional, comparative, and consecutive case–control study, 117 subjects (117 eyes) were prospectively evaluated, consisting of 34 healthy controls, 59 patients with DM without clinical signs of DR (noDR group) and 24 patients with mild nonproliferative DR (DR group). The right eye was included in the study. In case of artifacts or poor quality in the right eye images, the left eye was used. All patients with DM were enrolled from the Medical Retina service of the University Hospital Maggiore della Carità in Novara. Inclusion criteria were patients over age 18 with DM (type 1 and type 2, diagnosis confirmed by the diabetologist) without clinical signs of DR, or with mild nonproliferative DR according to the international classification (diagnosis made on slit-lamp fundus examination by the same ophthalmologist, SV, and documented on color fundus photograph of the macula)[38]; healthy subjects (with normal glucose test, control group); no history of ocular hypertension (IOP $<$ 21 mm Hg), nor neurodegenerative disease (e.g., multiple sclerosis, Alzheimer disease, Parkinson, etc). Major exclusion criteria were previous intraocular treatment (laser, intravitreal injections, and vitreoretinal surgery); cataract surgery within 6 months; any topical therapy; refractive error greater than +4 diopters (D); moderate or severe DR or diabetic macular edema; smoking; ischemic heart disease; and significant media opacity that precluded good quality fundus imaging and examination. For both controls and DM patients, series of examinations were performed, beginning with taking blood pressure measurements, collecting anamnestic data, including type of DM, recording the value of glycated hemoglobin (HbA1c), and performing a complete ophthalmologic examination with best-corrected visual acuity determination, IOP measurement, slit-lamp fundus examination in mydriasis with 90-D lens (for grading the absence/presence of DR), and color fundus photograph of the macula. On the same day, OCT and OCT-A exams were performed in mydriasis. This study followed the tenets of the Declaration of Helsinki and was approved by the institutional ethics committee. Signed informed consent was obtained from all patients.

Imaging

Spectral-Domain Optical Coherence Tomography and Optical Coherence Tomography Angiography. OCT and OCT-A images were taken using a swept-source OCT, DRI OCT Triton plus (Topcon Medical Systems Europe, Milano, Italy). This instrument uses 1050-nm wavelength light, with a scanning speed of 100,000 A-scans/second. The following three types of scans were performed: an OCT three-dimensional (3D) disc map covering an area of 6 × 6 mm centered on the papilla, an OCT-A maps covering 4.5 × 4.5 mm area centered on the papilla, and a 3 × 3-mm area centered on the fovea.

Spectral-Domain Optical Coherence Tomography Segmentation and Measurement. Using the 3D disc scan, peripapillary NFL thickness was measured by automated placement and scanning of a circle with 3.4 mm in diameter, centered on the papilla. Average thicknesses of total peripapillary NFL and superior, inferior, nasal, and temporal quadrants were determined with automatic segmentation with DRI OCT Triton plus OCT instrument (software version 10.07.003.03).

Optical Coherence Tomography Angiography Scans Evaluation. Peripapillary and macular OCT-A scans were used for quantitative evaluations. Peripapillary evaluation was performed at the level of the radial peripapillary capillary plexus (RPC); the macular evaluation was performed at the level of the superficial capillary plexus (SCP). The built-in software segmentation algorithm was used to define RPC and SCP on en face OCT angiograms. The RPC slab was obtained from the top of internal limiting membrane (ILM) to 70.2 μm below it. The SCP slab was obtained from the ILM to 15.6 μm above the inner plexiform layer/inner nuclear layer (IPL/INL) interface. Images with artifacts and those with signal strength index below 50 were excluded. Only good quality images were considered.

Quantitative peripapillary and macular parameters included the following: (1) perfusion density (PD; the total area occupied by the vessels); (2) vessel density (VD; the relative value of the total length of the vessels); and Branch analysis of skeletonized images, in particular (3) the number of branches (NoB), and (4) total branches length (tBL). All these parameters were evaluated with ImageJ version 1.51 software (http://imagej.nih.gov/ij/; provided in the public domain by the National Institutes of Health, Bethesda, MD, USA).[35,39–41]

ImageJ Analysis. OCT-A images were opened in ImageJ analysis software (Fig. 1). All OCT-A images were converted into 8-bit files (320 × 320 pixels; one-pixel macula ≈ 9.375 × 9.375 μm^2; one-pixel papilla ≈ 14.06 × 14.06 μm^2). All images underwent automatic "default" threshold available in the ImageJ software to neutralize the background noise. The image was then converted into a binarized black-and-white image. RPC slab images were analyzed eliminating the optic disc from the analysis (the region of interest was manually delineated by 2 evaluators and confirmed by the expert ophthalmologist) to remove the large vessels of the optic disc. This binary image was used to calculate PD (number of pixels of vessels/total pixels of the analyzed area).[39] The binarized image was used to create a skeletonized image to measure the statistical length of moving blood column, or VD [(number of pixels of vessels) × (scan width in mm/320) / (area in mm^2)], as previously described.[38] In this skeletonized image all vessels even large vessels are only one pixel wide. The skeletonized image was examined using Skeleton Analysis for the ImageJ application, AnalyzeSkeleton (Fig. 2). This plugin tags all pixels in a skeleton image, counts all their junctions, triple and quadruple points, and branches, and then measures average and maximum lengths.[40,41] When activating the plugin, a complementary results table called "branch information" is shown. From this automatic analysis we considered only two parameters, tBL and NoB.

In order to compare PD and VD with NFL thickness in each peripapillary quadrant (superior, inferior, nasal, and temporal), the binarized and skeletonized OCT-A images of the peripapillary region were divided into four quadrants, by two orthogonal lines, which crossed at the center of the papilla, using ImageJ. All images were saved and analyzed in anonymous and masked fashion.

Statistical Analysis

The clinical and demographic variables were compared among the three subject groups using one-way ANOVA for continuous variables and Fisher's exact test for categoric variables. Due to the relatively limited sample size in our study, we chose to consider baseline covariates (PA and age) in the analysis instead than in the patient selection phase. The variables which resulted significantly different among groups were considered as covariates in the following analyses, which were performed using analysis of covariance (ANCOVA), to compare clinical

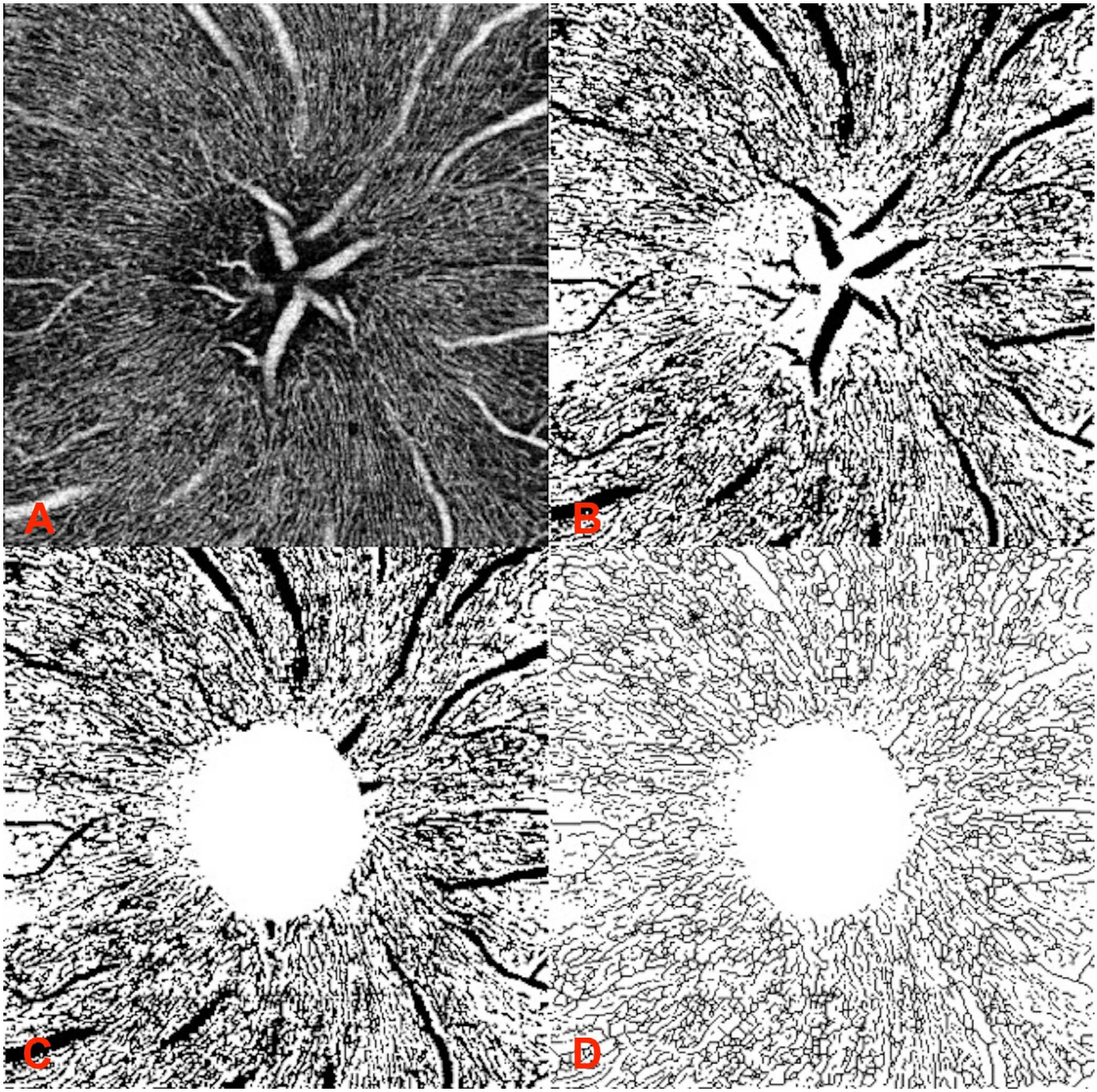

FIGURE 1. ImageJ analysis of the RPC image. (**A**) RPC slab image, (**B**) ImageJ binarization, (**C**) optic disc manually removed, and (**D**) ImageJ skeletonization.

variables among the three subject groups by adjusting for the level of the covariates.[42,43]

The means of populations were estimated as least squares means, which are the best linear estimates for the marginal means in the ANCOVA design. In case of an overall statistically significant ($P < 0.05$) or borderline significant difference among subject groups, pairwise comparisons among the three groups were done using the Scheffé test.[44] The correlation among nonnormally distributed variables were assessed using the Spearman's rank test and expressed through the nonparametric Spearman's correlation coefficient ρ. All the analyses were performed using Statistical version software 6.0 (StatSoft, Inc., Tulsa, OK, USA), using a two-sided type I error rate of $P = 0.05$.

RESULTS

Of 117 subjects (117 eyes, 100 were right eyes and 17 left eyes), 34 were healthy controls, 59 patients with DM without signs of DR, and 24 patients with mild-DR. In Table 1 represents patients' systemic characteristics (age, DM duration, HbA1c, systolic blood pressure, diastolic blood pressure, IOP, insulin treatment). Age and systolic blood pressure (SBP) showed statistically significant differences among the groups with ANOVA analysis. Table 2 shows values of NFL thickness in the peripapillary region (NFL average thickness and in each quadrant, superior, inferior, nasal, temporal). After adjusting for age and SBP there was a statistically significant difference in NFL thickness in the superior ($P = 0.025$) and inferior ($P =$

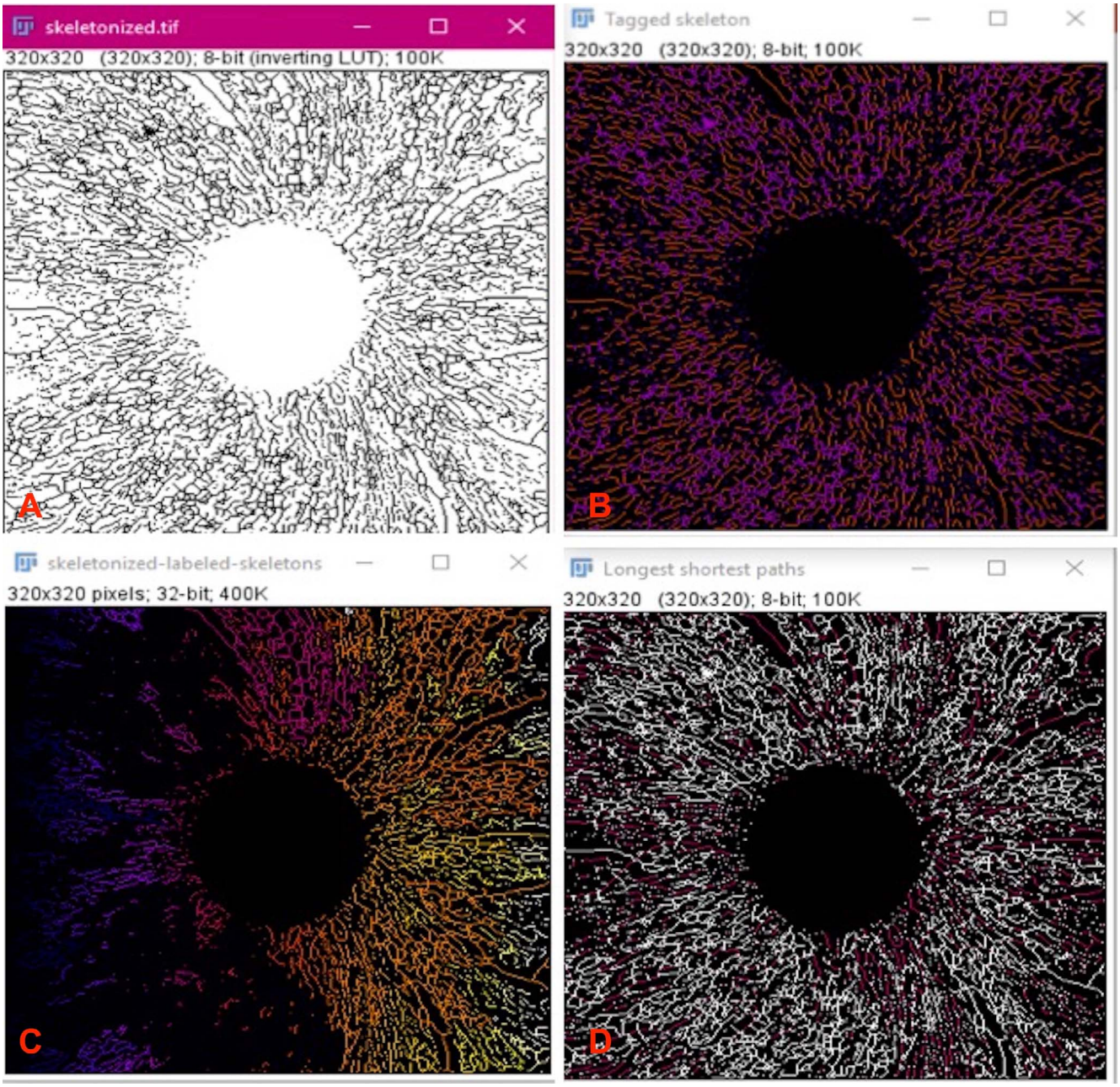

FIGURE 2. AnalyzeSkeleton analysis. Automatic analysis of skeletonized images. From this analysis the number of branches and branch's length can be counted. (**A**) Skeletonized Image with removed optic disc region that was analyzed with plugin AnalyzeSkeleton. (**B**) The plugin tagged pixels in the skeleton image (end-point pixels are displayed in *blue*, slab pixels in *orange* and junction pixels in *purple*). (**C**) An extra output image containing each skeleton labeled that corresponded to a skeleton ID from the associated table results (not shown). From the table, the number of branches and the total length of branches were determined. (**D**) Output image of the shortest (*magenta*) and the longest (*white*) path.

0.004) quadrants among the three groups. Pairwise comparisons evidenced significant differences between controls and DR in the superior quadrant ($P = 0.025$) and between controls and noDR ($P = 0.03$), and between noDR and DR ($P = 0.006$) in the inferior quadrant. Although not statistically significant, there was a clear trend of decreasing values for NFL average thickness from controls to noDR, and to DR ($P = 0.096$). Pairwise comparisons evidenced significant differences between controls and DR ($P = 0.008$). In the peripapillary region there was a trend of decreasing VD and PD values among controls, noDR and DR, although not reaching statistical significance (Table 3). Pairwise comparisons showed significant differences in VD between DR and noDR ($P = 0.03$) and between noDR and control ($P = 0.003$). NoB values in the peripapillary region showed a statistically significant decrease from control, to noDR and to DR ($P = 0.025$). Pairwise comparisons showed significant differences between control and noDR ($P < 0.001$) and between noDR and DR ($P = 0.03$). TBL values in the peripapillary region showed a decreasing trend from control to DR, although not statistically significant. Pairwise comparisons showed significant differences between control and noDR ($P < 0.001$) and between noDR and DR ($P = 0.003$). In the macular region there was a trend of decreasing PD and VD values among control, noDR and DR patients, almost reaching statistical significance (PD $P = 0.081$, VD $P = 0.058$). Pairwise comparisons showed significant differences in

Table 1. Sample Characteristic of the Subjects and Patients

Parameter	Controls ($N = 34$)	noDR ($N = 59$)	DR ($N = 24$)	ANOVA P Value*
Age, y	43.9 (11.9)	53.0 (18.9)	68.7 (12.3)	<0.001
DM duration, y	n.a.	10.5 (11.0)	11.2 (6.5)	0.77
HbA1c (%)	n.a.	6.8 (0.8)	6.9 (0.6)	0.81
SBP, mm Hg	130.1 (2.0)	138.3 (5.7)	141.8 (5.3)	<0.001
IOP, mm Hg	15.4 (2.3)	14.9 (2.1)	15.5 (2.1)	0.28
Insulin (% of patients)	n.a.	54.2	62.5	0.62†

Values are represented as mean (SD). n.a., not applicable.

* One-way ANOVA: comparison among controls, patients with DM without DR, and patients with DR.

† Fisher's Exact test was used. All patients with systemic hypertension were on lowering medication.

PD between DR and noDR ($P = 0.03$) and DR and controls ($P < 0.001$); in VD between DR and noDR ($P = 0.02$) and DR and controls ($P < 0.001$). Table 4 shows correlations between OCT-A parameters in the peripapillary region (PD, VD, NoB, and tBL) and NFL thickness values (average and separately in each quadrant). All the correlations were statistically significant with a Spearman's Rank Coefficient ρ ranging from a minimum value of 0.19 for the correlation between PD inferior (PDi) and NFL inferior (NFLi) and a maximum correlation of $\rho = 0.57$ for the correlation between VD and NFL average.

Discussion

In this study, we evaluated retinal capillary plexus in the most superficial layer (RPC) in the peripapillary region in healthy subjects and in patients with DM without DR and with mild nonproliferative DR using swept-source OCT-A. We found a significant decrease in VD, NoB and tBL in the peripapillary area in patients with DM, even without clinical signs of DR when compared with healthy subjects. PD values in the peripapillary region were not different among the groups. However, VD is considered to be more accurate parameter than PD in measuring retinal vascular changes, as the skeletonized image normalizes the diameter of larger vessels with that of capillaries, removing the influence of vessel size on retinal perfusion measurements.[35,39,45]

The PD and VD were also evaluated in the macular region in SCP, and both parameters were found decreased in patients with mild DR versus controls and in mild DR versus noDR group. In the macular region, only SCP was evaluated, in order to evaluate the most superficial vascular plexus in both areas. Moreover, SCP is considered more easily evaluated for differentiating healthy eyes from eyes with DR as previously reported.[46,47] The present data are in agreement with previously published data evaluating VD in the macular region and reporting a significant decrease in patients with DR versus healthy controls.[35,48] Some authors have described a decrease in VD even in patients with DM without DR versus control.[34,47] Lei et al.[47] evaluated only superficial capillaries on images having very different signal strength among groups, that might have influenced the analyses, as reported by the same authors. Dimitrova et al.[34] described a significant difference in macular VD between patients with DM without DR and healthy subjects. However, data from the present study cannot be directly compared with the data from Dimitrova et al.[34] due to differences in subjects' ethnicity (only Asian patients were included) number of evaluated subjects, duration of DM, and the use of different OCT-A machines.

Table 2. Values of NFL Thickness in the Peripapillary Region

Parameter	Controls ($N = 34$)	noDR ($N = 59$)	DR ($N = 24$)	ANCOVA P Value*
NFL				
Average	108.5 (9.0)	105.8 (11.8)	99.1† (12.6)	0.096
Superior	130.4 (12.6)	126.8 (17.5)	118.0‡ (21.3)	0.025
Inferior	139.1 (15.9)	134.8§ (18.7)	123.3‖ (19.0)	0.004
Nasal	85.5 (18.6)	84.4 (13.9)	82.5 (16.0)	0.769
Temporal	78.8 (12.7)	77.0 (14.8)	72.4 (10.4)	0.200

* ANCOVA analyses by adjusting for age and SBP: comparison among controls, patients with DM without DR, and patients with DR.

Comparison vs. controls:

† Scheffè test, $P = 0.008$.

‡ Scheffè test, $P = 0.025$.

§ Scheffè test, $P = 0.03$.

Comparison vs. patients with DM without DR:

‖ Scheffè test, $P = 0.006$.

Currently, there is no available OCT-A data on peripapillary VD in patients with DM in the literature. We found a significant decrease in VD in the peripapillary region even in patients without DR while, in macular region, this decrease was found only when clinical signs of DR were present. This could indicate that peripapillary microvascular alterations in VD occur earlier than in the macular region, even before the appearance of clinically visible signs of DR; consequently, changes in RPC in the peripapillary region could represent an early preclinical sign of diabetic microvascular disease. This could be explained due to the peculiar anatomic conformation of the peripapillary plexus,[21] made up of capillaries with long straight paths and rare anastomotic connections, remaining strictly associated with NFL, and giving important nourishment to the NFL in this region. These features differentiate RPC from SCP in the macular region, that forms a dense capillary network with numerous anastomoses also with the underlying plexuses (intermediate and deep capillary plexuses).[21,23,24]

The present work documents a significant reduction in NoB and tBL in patients with DM without signs of DR when compared with healthy subjects in the peripapillary region. This is the first study that evaluates retinal vasculature parameters with the aid of ImageJ plug-in, AnalyzeSkeleton. Previous studies have demonstrated the importance and reproducibility of this method of analysis for the automatic reconstruction of biological tissues in order to provide morphologic phenotype information, but none of these studies used AnalyzeSkeleton to evaluate retinal vascularization.[40,41] Arganda-Carreras et al.[40] previously described the process of the algorithm of ImageJ plug-in, AnalyzeSkeleton. The system of analysis is completely automatic and shows all branches of retinal vessels and their length, giving morphologic information about retinal vascularization and its modifications in retinal diseases.

Given the fractal nature of retinal vascularization, many authors have tried to study its features using fractal analysis, that calculates the so-called fractal dimension (FD), a mathematic parameter that describes the complexity of a biological structure, such as branching angle, tortuosity, and vessel complexity.[49–51] Different authors have demonstrated alterations of FD in patients with DR using color and red-free fundus photographs and fluorescein angiography.[52–55] These authors evaluated only large retinal vessels reporting both increased and decreased FD in DR. However, the previously mentioned technology did not allow for evaluation of morphologic changes at the capillary level, which can be easily evaluated using OCT-A.[23] Recently, there has been several papers on evaluation of vessel FD in the macular region using OCT-A in patients with DM.[35,39,56,57] Reif et al.[39]

Table 3. Quantitative OCT-A Parameters in the Peripapillary and Macular Regions

Parameter	Controls ($N = 34$)	noDR ($N = 59$)	DR ($N = 24$)	ANCOVA P Value*
PD				
Peripapillary	0.37 (0.03)	0.35 (0.03)	0.33† (0.05)	0.126
Macular	0.31 (0.04)	0.29 (0.03)	0.27‡** (0.02)	0.081
VD				
Peripapillary	0.20 (0.01)	0.18§ (0.02)	0.17†† (0.03)	0.132
Macular	0.15 (0.03)	0.14 (0.01)	0.12‖‡‡ (0.01)	0.058
NoB	202.1 (11.4)	189.0¶ (17.8)	117.4** (34.8)	0.025
tBL	344639 (65016)	299644# (49931)	274465§§ (73692)	0.142

* ANCOVA analyses by adjusting for age and SBP: comparison among controls patients with DM without DR, and patients with DR.
Comparison vs. controls:
† Scheffè test, $P < 0.001$.
‡ Scheffè test, $P < 0.001$.
§ Scheffè test, $P = 0.003$.
‖ Scheffè test, $P < 0.001$.
¶ Scheffè test, $P < 0.001$.
# Scheffè test, $P < 0.001$.
Comparison vs. patients with DM without DR:
** Scheffè test, $P = 0.03$.
†† Scheffè test, $P = 0.03$.
‡‡ Scheffè test, $P = 0.02$.
§§ Scheffè test, $P = 0.003$.

were the first to describe capillary FD with a prototype OCT-A in an mouse ear model. Other authors described a decrease in FD in patients with DM (type 1 and type 2) from mild DR to proliferative DR.[35,56] As FD geometry mirrors the physiologic branching of the retinal vascular tree, the FD may provide better insights into pathogenesis of DR. Moreover, FD used with other quantitative analyses (such as VD, areas of nonperfusion, etc.) may help for disease risk stratification, and evaluation of treatment. Chen et al.[57] evaluated FD in patients with DM without DR in the macula and found a significant decrease versus healthy controls. Moreover, this reduction was significant only in the deep capillary plexus. This may be due to specific anatomy of the DCP (greater density of smaller vessels in the DCP versus SCP), in which vascular constriction of the DCP in the macular region may be an earlier compensating mechanism than in the SCP for decreased blood flow and resulting hypoxia and ischemia in patients with DM.[57]

Table 4. Correlations Between OCT-A Parameters in the Peripapillary Region (PD, VD, NoB, and tBL) and NFL Thickness Values (Average and Separately in Each Quadrant)

	NFL				
Parameter	Average	Superior	Inferior	Nasal	Temporal
All subjects					
PD	0.43*				
PDs		0.34*			
PDi			0.19*		
PDn				0.26*	
PDt					0.40*
VD	0.57*				
VDs		0.43*			
VDi			0.34*		
VDn				0.30*	
VDt					0.44*
tBL	0.47*				
NoB	0.48*				

s, superior; i, inferior; n, nasal; t, temporal.
* Spearman's rank coefficient.

Even if performed with a different method of analysis and in a different retinal region (peripapillary area), the present data confirm the importance of vessel morphology evaluation in the study of patients with DM before the appearance of clinical signs of DR. Further longitudinal studies would be necessary to compare the present data obtained with AnalyzeSkeleton with peripapillary fractal analysis, never performed before in this region in patients with DM, in order to define if the number of branches is more predictive of DR development than complexity of capillaries.

Previously, both experimental and clinical studies have reported on the presence of early neurodegeneration in the retina in patients with DM without clinical signs of DR.[3,4,13–15,58] In the present study, we found a significant decrease in average NFL thickness and in the superior quadrant of patients with DR versus controls. Instead, very early reduction in NFL thickness was found in the inferior quadrant, even in patients with DM without DR versus controls. These data agree with recent clinical works on peripapillary average NFL thickness in patients with DM and with or without DR.[14,59]

In the present study, there is a significant correlation between OCT-A parameters (PD, VD, NoB, and tBL) and NFL thickness values (average and separately in each quadrant) in the peripapillary region. These data are in agreement with previous postmortem histologic studies that described a correlation between RPC volume and NFL thickness in healthy human donor retinas.[22] Mase et al.[26] described this correlation in healthy subjects using OCT-A, suggesting that RPC is the most important structure in maintaining NFL integrity. The decrease and correlations among OCT-A parameters and NFL thickness in the peripapillary region may confirm a coexistence of an early neuronal and microvascular damage in patients with DM without clinical signs of DR. The exact relationship (including also the temporal one) between the neuronal and the microvascular damage remains to be further evaluated, and certainly confirms the need to move beyond the pure microvascular classification of DR and to integrate also neuronal damage into classification of diabetic retinal disease.[60]

The major limitation of this study includes a cross-sectional design without longitudinal data especially in determining the

prognostic value of the evaluated parameters for development of DR. The pairwise comparisons tests employed were already designed to control familywise error rates in the absence of any significant prior omnibus analysis. However, we chose to run the pairwise comparisons only in the case of overall significance or borderline significance as an over protection against potential type I error. We acknowledge that given the small study with multiple comparisons, the potential of having false-positive results may still exist and therefore the results should be considered more as an insight provided to the reader with preliminary data, than a definitive conclusion that would need further confirmation from larger studies.

In conclusion, this study documents very early changes in the peripapillary vessel density and morphology (VD, NoB, tBL) of the most superficial capillary plexus (RPC) in patients with DM without DR and correlate it to NFL thinning. Earlier changes in superficial vessel density are documented in the peripapillary region than in the macular region. Specific anatomic characteristics of the RPC may be responsible of greater and earlier microvascular susceptibility to chronic hyperglycemia in DM, then in the macular region. Further, longitudinal studies linking all these evaluated OCT-A parameters to the neuronal damage (such as thinning of the NFL) might help in better understanding of microvascular and neuronal relationship in DM and in finding a predictive marker of DR development.

Acknowledgments

The authors thank Caterina Toma, MD, and Chiara Nutini, MS, for their help in collecting data.

Disclosure: **S. Vujosevic**, None; **A. Muraca**, None; **V. Gatti**, None; **L. Masoero**, None; **M. Brambilla**, None; **B. Cannillo**, None; **E. Villani**, None; **P. Nucci**, None; **S. De Cillà**, None

References

1. Yau JWY, Rogers SL, Kawasaki R, et al. Global prevalence and major risk factors of diabetic retinopathy. *Diabetes Care*. 2012;35:556–564.
2. Joussen AM, Poulaki V, Qin W, et al. Retinal vascular endothelial growth factor induces intercellular adhesion molecule-1 and endothelial nitric oxide synthase expression and initiates early diabetic retinal leukocyte adhesion in vivo. *Am J Pathol*. 2002;160:501–509.
3. Martin PM, Roon P, Van Ells TK, Ganapathy V, Smith SB. Death of retinal neurons in streptozotocin-induced diabetic mice. *Invest Ophthalmol Vis Sci*. 2004;45:3330–3336.
4. Lecleire-Collet A, Tessier LH, Massin P, et al. Advanced glycation end products can induce glial reaction and neuronal degeneration in retinal explants. *Br J Ophthalmol*. 2005;89:1631–1633.
5. Antonetti DA, Barber AJ, Bronson SK, et al. Diabetic retinopathy: seeing beyond glucose-induced microvascular disease. *Diabetes*. 2006;55:2401–2411.
6. Vujosevic S, Micera A, Bini S, Berton M, Esposito G, Midena E. Aqueous humor biomarkers of müller cell activation in diabetic eyes. *Invest Ophthalmol Vis Sci*. 2015;56:3913–3918.
7. Vujosevic S, Micera A, Bini S, Berton M, Esposito G, Midena E. Proteome analysis of retinal glia cells-related inflammatory cytokines in the aqueous humour of diabetic patients. *Acta Ophthalmol*. 2016;94:56–64.
8. Antonetti DA, Klein R, Gardner TW. Diabetic retinopathy. *N Engl J Med*. 2012;366:1227–1239.
9. Das A, McGuire PG, Rangasamy S. Diabetic macular edema: pathophysiology and novel therapeutic targets. *Ophthalmology*. 2015;122:1375–1394.
10. Simó R, Hernández C; for the European Consortium for the Early Treatment of Diabetic Retinopathy (EUROCONDOR). Neurodegeneration in the diabetic eye: new insights and therapeutic perspectives TL - 25. *Trends Endocrinol Metab*. 2014;25:23–33.
11. Stem MS, Gardner TW. Neurodegeneration in the pathogenesis of diabetic retinopathy: molecular mechanisms and therapeutic implications. *Curr Med Chem*. 2013;20:3241–3250.
12. Cabrera DeBuc D, Somfai GM. Early detection of retinal thickness changes in diabetes using optical coherence tomography. *Med Sci Monit*. 2010;16:MT15–MT21.
13. Park HY-L, Kim IT, Park CK. Early diabetic changes in the nerve fibre layer at the macula detected by spectral domain optical coherence tomography. *Br J Ophthalmol*. 2011;95:1223–1228.
14. Vujosevic S, Midena E. Retinal layers changes in human preclinical and early clinical diabetic retinopathy support early retinal neuronal and Müller cells alterations. *J Diabetes Res*. 2013;2013:905058.
15. Chhablani J, Sharma A, Goud A, et al. Neurodegeneration in type 2 diabetes: evidence from spectral-domain optical coherence tomography. *Invest Ophthalmol Vis Sci*. 2015;56:6333–6338.
16. Gundogan FC, Akay F, Uzun S, Yolcu U, Çağlltay E, Toyran S. Early neurodegeneration of the inner retinal layers in type 1 diabetes mellitus. *Ophthalmologica*. 2016;235:125–132.
17. Carpineto P, Toto L, Aloia R, et al. Neuroretinal alterations in the early stages of diabetic retinopathy in patients with type 2 diabetes mellitus. *Eye*. 2016;30:673–679.
18. El-Fayoumi D, Badr Eldine NM, Esmael AF, Ghalwash D, Soliman HM. Retinal nerve fiber layer and ganglion cell complex thicknesses are reduced in children with type 1 diabetes with no evidence of vascular retinopathy. *Invest Opthalmology Vis Sci*. 2016;57:5355–5360.
19. Vujosevic S, Muraca A, Alkabes M, et al. Early microvascular and neural changes in patients with type 1 and type 2 diabetes mellitus without clinical signs of diabetic retinopathy [published online ahead of print December 4, 2017]. *Retina*. doi: 10.1097/IAE.0000000000001990.
20. Zheng Y, Cheung N, Aung T, Mitchell P, He M, Wong TY. Relationship of retinal vascular caliber with retinal nerve fiber layer thickness: the Singapore Malay Eye Study. *Invest Ophthalmol Vis Sci*. 2009;50:4091–4096.
21. Henkind P. Symposium on Glaucoma: joint meeting with the National Society for the Prevention of Blindness: new observations on the radial peripapillary capillaries. *Invest Ophthalmol Vis Sci*. 1967;6:103–108.
22. Yu PK, Cringle SJ, Yu DY. Correlation between the radial peripapillary capillaries and the retinal nerve fibre layer in the normal human retina. *Exp Eye Res*. 2014;129:83–92.
23. Spaide R, Klancnik J, Cooney M. Retinal vascular layers imaged by fluorescein angiography and optical coherence tomography angiography. *JAMA Ophthalmol*. 2015;133:45–50.
24. Spaide RF, Fujimoto JG, Waheed NK, Sadda SR, Staurenghi G. Optical coherence tomography angiography. *Prog Retin Eye Res*. 2018;64:1–55.
25. Rabiolo A, Carnevali A, Bandello F, Querques G. Optical coherence tomography angiography: evolution or revolution? *Expert Rev Ophthalmol*. 2016;11:243–245.
26. Mase T, Ishibazawa A, Nagaoka T, Yokota H, Yoshida A. Radial peripapillary capillary network visualized using wide-field montage optical coherence tomography angiography. *Invest Ophthalmol Vis Sci*. 2016;57:504–510.
27. Yu PK, Balaratnasingam C, Xu J, et al. Label-free density measurements of radial peripapillary capillaries in the human retina. *PLoS One*. 2015;10:e0135151.

28. Lee EJ, Lee KM, Lee SH, Kim TW. Oct angiography of the peripapillary retina in primary open-angle glaucoma. *Invest Ophthalmol Vis Sci*. 2016;57:6265–6270.
29. Mammo Z, Heisler M, Balaratnasingam C, et al. Quantitative optical coherence tomography angiography of radial peripapillary capillaries in glaucoma, glaucoma suspect, and normal eyes. *Am J Ophthalmol*. 2016;170:41–49.
30. Mansoori T, Sivaswamy J, Gamalapati JS, Balakrishna N. Radial peripapillary capillary density measurement using optical coherence tomography angiography in early glaucoma. *J Glaucoma*. 2017;26:438–443.
31. Yarmohammadi A, Zangwill LM, Diniz-Filho A, et al. Optical coherence tomography angiography vessel density in healthy, glaucoma suspect, and glaucoma eyes. *Invest Ophthalmol Vis Sci*. 2016;57:451–459.
32. Triolo G, Rabiolo A, Shemonski ND, et al. Optical coherence tomography angiography macular and peripapillary vessel perfusion density in healthy subjects, glaucoma suspects, and glaucoma patients. *Invest Ophthalmol Vis Sci*. 2017;58:5713–5722.
33. Liu L, Jia Y, Takusagawa HL, et al. Optical coherence tomography angiography of the peripapillary retina in glaucoma. *JAMA Ophthalmol*. 2015;133:1045–1052.
34. Dimitrova G, Chihara E, Takahashi H, Amano H, Okazaki K. Quantitative retinal optical coherence tomography angiography in patients with diabetes without diabetic retinopathy. *Invest Ophthalmol Vis Sci*. 2017;58:190–196.
35. Kim AY, Chu Z, Shahidzadeh A, Wang RK, Puliafito CA, Kashani AH. Quantifying microvascular density and morphology in diabetic retinopathy using spectral-domain optical coherence tomography angiography. *Invest Ophthalmol Vis Sci*. 2016;57:362–370.
36. Sandhu HS, Eladawi N, Elmogy M, et al. Automated diabetic retinopathy detection using optical coherence tomography angiography: a pilot study [published online ahead of print January 23, 2018]. *Br J Ophthalmol*. doi:10.1136/bjoph thalmol-2017-311489.
37. Kim K, Kim ES, Yu S-Y. Optical coherence tomography angiography analysis of foveal microvascular changes and inner retinal layer thinning in patients with diabetes. *Br J Ophthalmol*. 2018;102:1226–1231.
38. Global Diabetic Retinopathy Project Group. Proposed international clinical diabetic retinopathy and diabetic macular edema disease severity scale. *Ophthalmology*. 2003;110:1677–1682.
39. Reif R, Qin J, An L, Zhi Z, Dziennis S, Wang R. Quantifying optical microangiography images obtained from a spectral domain optical coherence tomography system. *Int J Biomed Imaging*. 2012;2012:509783.
40. Arganda-Carreras I, Fernández-González R, Muñoz-Barrutia A, Ortiz-De-Solorzano C. 3D reconstruction of histological sections: application to mammary gland tissue. *Microsc Res Tech*. 2010;73:1019–1029.
41. Polder G, Hovens HLE, Zweers AJ, Jahnen A, Moll C, Kennedy AJF. Measuring shoot length of submerged aquatic plants using graph analysis. *Proc ImageJ User Dev Conf*. 2010:172–177.
42. Pocock SJ, Assmann SE, Enos LE, Kasten LE. Subgroup analysis, covariate adjustment and baseline comparisons in clinical trial reporting: current practice and problems. *Stat Med*. 2002;21:2917–2930.
43. Kahan BC, Jairath V, Doré CJ, Morris TP. The risks and rewards of covariate adjustment in randomized trials: an assessment of 12 outcomes from 8 studies. *Trials*. 2014;15:139.
44. Howell DC. *Statistical Methods for Psychology*. 8th ed. Belmont, CA: Cengage Wadsworth. 2013.
45. Ghasemi Falavarjani K, Al-Sheikh M, Darvizeh F, Sadun AA, Sadda SR. Retinal vessel calibre measurements by optical coherence tomography angiography. *Br J Ophthalmol*. 2017;101:989–992.
46. Durbin MK, An L, Shemonski ND, et al. Quantification of retinal microvascular density in optical coherence tomographic angiography images in diabetic retinopathy. *JAMA Ophthalmol*. 2017;135:370–376.
47. Lei J, Yi E, Suo Y, et al. Distinctive analysis of macular superficial capillaries and large vessels using optical coherence tomographic angiography in healthy and diabetic eyes. *Invest Ophthalmol Vis Sci*. 2018;59:1937–1943.
48. Agemy SA, Scripsema NK, Shah CM, et al. Retinal vascular perfusion density mapping using optical coherence tomography angiography in normals and diabetic retinopathy patients. *Retina*. 2015;35:2353–2363.
49. Lakshminanarayanan V, Raghuram A, Myerson JW, Varadharajan S. The fractal dimension in retinal pathology. *J Mod Opt*. 2003;50:1701–1703.
50. Masters BRB. Fractal analysis of the vascular tree in the human retina. *Annu Rev Biomed Eng*. 2004;6:427–452.
51. Liew G, Wang JJ, Cheung N, et al. The retinal vasculature as a fractal: methodology, reliability, and relationship to blood pressure. *Ophthalmology*. 2008;115:1951–1956.
52. Talu S, Calugaru DM, Lupascu CA. Characterisation of human non-proliferative diabetic retinopathy using the fractal analysis. *Int J Ophthalmol*. 2015;8:770–776.
53. Grauslund J, Green A, Kawasaki R, Hodgson L, Sjolie AK, Wong TY. Retinal vascular fractals and microvascular and macrovascular complications in type 1 diabetes. *Ophthalmology*. 2010;117:1400–1405.
54. Cheung N, Donaghue KC, Liew G, et al. Quantitative assessment of early diabetic retinopathy using fractal analysis. *Diabetes Care*. 2009;32:106–110.
55. Avakian A, Kalina RE, Helene Sage E, et al. Fractal analysis of region-based vascular change in the normal and non-proliferative diabetic retina. *Curr Eye Res*. 2002;24:274–280.
56. Zahid S, Dolz-Marco R, Freund KB, et al. Fractal dimensional analysis of optical coherence tomography angiography in eyes with diabetic retinopathy. *Invest Opthalmol Vis Sci*. 2016;57:4940–4947.
57. Chen Q, Ma Q, Wu C, et al. Macular vascular fractal dimension in the deep capillary layer as an early indicator of microvascular loss for retinopathy in type 2 diabetic patients. *Invest Ophthalmol Vis Sci*. 2017;58:3785–3794.
58. Villarroel M, Ciudin A, Hernández C, Simó R. Neurodegeneration: an early event of diabetic retinopathy. *World J Diabetes*. 2010;1:57–64.
59. Pierro L, Iuliano L, Cicinelli MV, Casalino G, Bandello F. Retinal neurovascular changes appear earlier in type 2 diabetic patients. *Eur J Ophthalmol*. 2017;27:346–351.
60. Abramoff MD, Fort PE, Han IC, Thiran Jayasundera K, Sohn EH, Gardner TW. Approach for a clinically useful comprehensive classification of vascular and neural aspects of diabetic retinal disease. *Invest Ophthalmol Vis Sci*. 2018;59:519–527.

Investigative Ophthalmology & Visual Science